# NOTICE CONCERNING COPYRIGHT RESTRICTIONS

# The Coso EGS Project—Recent Developments

**Peter Rose[1], Colleen Barton[2], Jess McCulloch[3], Joseph N. Moore[1], Katie Kovac[1], Judith Sheridan[2], Paul Spielman[3], and Brian Berard[3]**

**[1]Energy and Geoscience Institute at the University of Utah**
**423 Wakara Way suite 300, Salt Lake City, Utah 84108**
**[2]Geomechanics International, 250 Cambridge Ave. Suite 103, Palo Alto, CA 94306**
**[3]Coso Operating Company, Coso Junction, CA 93542**

***Keywords***

*Enhanced Geothermal Systems, reservoir stress, reservoir stimulation, borehole image analysis*

## ABSTRACT

A preliminary fracture/stress analysis was conducted for the recently drilled well 38C-9 as part of a continuing effort to characterize the stress state within the east flank of the Coso geothermal field. Electric Micro Imager (EMI) data were analyzed over the logged interval of 5,881-9,408 ft. Naturally occurring fractures were analyzed in order to determine both fracture dip and azimuth. Most of the fractures dip steeply with dip azimuths approximately to the east, with a subset dipping steeply in a westerly direction. Drilling induced tensile fractures were used to determine that the orientation of the maximum horizontal stress is 14° +/- 16°, although this is approximate as the data have to be corrected for wellbore deviation. Petrologic analyses of cuttings from several wells were used to construct a vein-mineral paragenesis of the Coso east flank. Fluid inclusion analyses of cuttings from well 83-16 were used to determine the temperatures of vein mineralization.

## Introduction

The east flank of the Coso geothermal field is an excellent setting for testing Enhanced Geothermal System (EGS) concepts (see Figure 1). Fluid temperatures exceeding 300°C have been measured at depths less than 10,000 ft and the reservoir is both highly fractured and tectonically stressed. However, some of the wells within this portion of the reservoir are relatively impermeable. High rock temperatures, a high degree of fracturing, high tectonic stresses and low permeability are the qualities that define an ideal candidate-EGS reservoir. With a grant from DOE, we have therefore assembled a team of scientists and engineers from Coso Operating Company, Geomechanics International (GMI), the Navy Geothermal Program Office, the USGS, Kansas State University, the Energy and Geoscience Institute and elsewhere for the purpose of developing and evaluating an approach for the creation of an EGS within the Coso east flank reservoir.

Key to the creation of an EGS is an understanding of the relationship among natural fracture distribution, fluid flow and the ambient tectonic stresses that exist within the resource. Once these relationships are determined, we will proceed to design a hydraulic and thermal stimulation of an east-flank injection well as the first step in the creation of a heat exchanger at depth. We will quantify the success of our experiment through hydraulic,

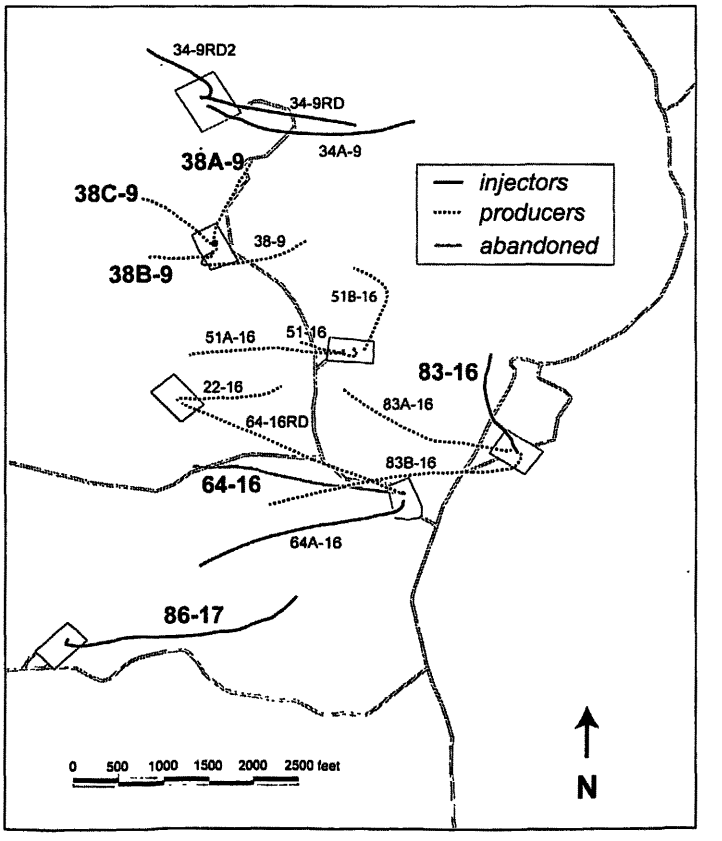


**Figure 1.** Locations and trajectories of wells within the east flank EGS study area of the Coso geothermal field.

microseismic, geomechanical, and geochemical measurements. Finally, we will drill a production well within the east-flank region in order to create the heat-exchanger doublet that will comprise the heart of the EGS.

## The Coso/EGS Program Objectives and Approach

The overarching objective of the Coso/EGS project is to design and create an Enhanced Geothermal System within the east flank of the Coso geothermal field. The EGS will consist of one or more low permeability injection wells that will be stimulated through a combination of hydraulic, thermal and chemical methods and connected to at least one production well.

Our objective is not only to design and demonstrate an EGS on the periphery of an existing geothermal reservoir, but to understand the processes that control permeability enhancement. The primary analytical tools that we will use include borehole logs to image fractures and determine regional stresses, petrographic and petrologic analyses of borehole cuttings, petrophysical measurements of core samples, geophysical methods including microseismology and magneto-telluric (MT) studies, structural analysis, fluid-flow modeling, and geochemical modeling. We believe lessons learned at Coso will make it possible to design and create an EGS wherever appropriate tectonic, thermal and hydraulic conditions exist, thereby allowing geothermal operators to greatly extend their developmental reach beyond the relatively few high grade hydrothermal resources.

We are nearing the end of the second year of this 5-year, EGS project. The first year consisted of an analysis of existing data in order to characterize the stress state of the Coso east flank and to identify candidate injection wells for hydraulic, thermal and chemical stimulation. During the second year of the project, a production well was drilled that will serve as the production half of an EGS injector/producer doublet. During the remaining three years of the program, one or more injection wells will be redrilled and stimulated and a circulation test will be conducted in order to demonstrate an EGS within the east flank of the Coso geothermal system. This project is funded by the Department of Energy with matching funding from Coso Operating Company.

## Preliminary Fracture and Wellbore Failure Analysis in Coso Well 38C-9

A fracture/stress analysis of four wells in the Coso east flank study area was recently published (Sheridan et al, 2003). In this paper, we present a preliminary facture and wellbore failure analysis of east flank well 38C-9, which was drilled and completed since that paper was published.

### *Background and Theory*

Barton et al. (1995, 1998) have shown that optimally oriented, critically stressed fractures control permeability in areas of active tectonism. This suggests that critically stressed fracture sets are likely to be responsible for the majority of the geothermal production in the Coso geothermal field. Knowledge of the local stress tensor is needed to determine the proximity of natural fractures to frictional failure and therefore, to determine their role in controlling reservoir permeability. A detailed analysis is required in order to develop a geomechanical model of the reservoir and to determine which fractures are optimally oriented and critically stressed for shear failure. The geomechanical model includes the pore pressure ($P_p$), the uniaxial compressive rock strength ($C_0$), and the magnitudes and orientations of the most compressive ($S_1$), intermediate ($S_2$), and least compressive ($S_3$) principal stresses. These are derived from *in situ* pore pressure measurements, laboratory rock strength tests, wireline log data, minifrac test results and observations of wellbore failure. Only through fracture and wellbore failure analyses of image data, correlated petrographic analyses, and identification of critically stressed faults can the effects of subsequent stimulation experiments be understood.

We have interpreted the natural and drilling-induced features in the Electric Micro Imager (EMI) image data from the Coso wells. Planar structural features that intersect the borehole appear as sinusoids on unwrapped 360° views of the image data. These sinusoids are often discontinuous for fine-scale fractures and can show very complex patterns at points where several fractures intersect or where fractures are not perfectly planar. The digital analysis of planar features is accomplished interactively using a fracture measurement tool, a flexible sinusoid that is fit to the trace of fracture plane in the image. Once the feature is selected, the depth, true dip and dip direction, and apparent dip and dip direction of the feature are calculated and recorded.

Stress-induced wellbore breakouts occur when the compressive stress concentration around the borehole wall exceeds the rock strength. The presence, orientation and severity of failure are a function of the in situ stress field, the wellbore orientation and the rock strength (Zoback et al., 1985; Moos and Zoback, 1992). In a vertical well in a region where overburden is a principal stress, breakouts may form on opposite sides of the wellbore at the azimuth of the minimum horizontal far-field compression, as this is where the compressive hoop stress is greatest.

Drilling-induced tensile fractures occur in the borehole wall where the circumferential hoop stress is negative and exceeds the tensile strength of the rock. These fine-scale features occur only in the wall of the borehole (due to the localized stress concentration) and do not propagate away from the hole. These fractures form either parallel to the borehole axis or, in the case in which the borehole axis is not parallel to one of the principal stresses (e.g., in deviated wellbores), in *en echelon* patterns with the fracture planes inclined to the borehole axis (Peska and Zoback, 1995).

Both excess mud weight and wellbore cooling can influence the occurrence of drilling-induced tensile wall fractures. It is clear that both cause a component of tensile stress to be added to the hoop stress acting around the wellbore and can play a role in the formation of tensile fractures. The role of excess mud weight is fairly obvious—the decrease in hoop stress is simply proportional to the excess mud weight. The effect at the wellbore wall of a temperature difference ($\Delta T$) between the wellbore fluid and the rock surrounding the well is given by the following equation:

$$\sigma_{\theta\theta}^{\Delta T} = (\alpha E \Delta T)/(1 - \nu)$$

where $\alpha$ is the linear coefficient of thermal expansion and E is

Young's modulus (Moos and Zoback, 1990). The thermal stress at the borehole wall is therefore proportional to both the amount of cooling and the physical properties of the rock. In many geothermal wells, wellbore cooling (which can be on the order of 100° C) can be the major cause of drilling-induced tensile wall fractures—both because the temperature difference is large and because such wells are often drilled into rocks with very high elastic moduli.

## *Analysis of Well 38C-9*

EMI data were analyzed over a logged interval 5,881–9,408 ft MD in well 38C-9. The EMI tool provides good data for detecting macroscopic fractures that intersect the wellbore and cut across lithologic contacts. Planar features detected in electrical image data are the result of the electrical conductivity contrast between the feature and the host rock. Consequently, it is sometimes difficult to distinguish between foliation, flow banding, bedding, and natural fractures in electrical image data. For this reason, populations of planar features detected through electrical imaging can represent a large variety of features.

The extremely high density of natural fractures in 38C-9 tends to obscure drilling-induced tensile fractures in the image logs. Extreme care was therefore used to discriminate between drilling-induced and naturally occurring fractures. In some intervals in the image logs it was not possible to discern between the population of sub-vertical natural fractures and drilling-induced fractures. In other depth intervals, however, many drilling-induced fractures are discriminated from natural fractures.

Figure 2 shows the results of a preliminary analysis of EMI logs for well 38C-9 over the interval 5,881–9,408 ft. Figures 2a and 2b show fracture dip and dip azimuth, respectively, with each point representing a distinct fracture. Figure 2c shows fracture frequency or the number of fractures per foot measured over the interval. The final column in Figure 2 shows the EMI data quality as a function of depth.

Recently acquired image logs for the deeper portion of well 38C-9 were analyzed for the distribution and orientation of drilling-induced tensile wall failure. Tensile failure occurs in discrete intervals throughout the logged section. However, Coso wells are intensely fractured and the abundance of high-angle natural fractures makes discrimination of these induced features from high-angle natural fractures extremely difficult. In many cases, tensile wall fractures are observed as being rotated to a non-axial position due to their proximity to natural fractures. The natural fractures give rise to a localized free surface which can result in a perturbation of the stresses resolved on the wellbore wall, subsequently causing tensile wall fractures to propagate non-axially along the borehole wall.

To avoid contamination of the tensile wall fracture analysis from these local perturbations of the stress field, strict criteria were used in the analysis of tensile wall fractures. First, tensile fractures must be axially aligned and unaffected by nearby natural fractures, and second, they must occur as a single pair at opposite sides of the wellbore wall (~180° apart). For wellbore deviations up to 12°, the azimuths of wellbore failures are approximately what they would be in a vertical borehole (Mastin, 1988). This is because one of the principal stress directions is usually vertical and therefore parallel to a near vertical wellbore. In this case tensile fractures are parallel to the $S_{Hmax}$. In a wellbore that is not parallel to one of the principal stress directions (wellbore deviation greater than 12°) the minimum and maximum stress magnitudes on the wellbore wall may be rotated away from the principal stress directions. In this case, additional stress modeling is required to determine the relationship between tensile fractures and $S_{Hmax}$ azimuth. For this reason, these preliminary results provide only the orientation of tensile fractures observed in the deeper logged interval in Coso 38C-9 and not necessarily the precise $S_{Hmax}$ orientation.

Wellbore failure was observed over the interval 5,881–9,408 feet in well 38C-9. Drilling-induced tensile fractures were observed in these image data.

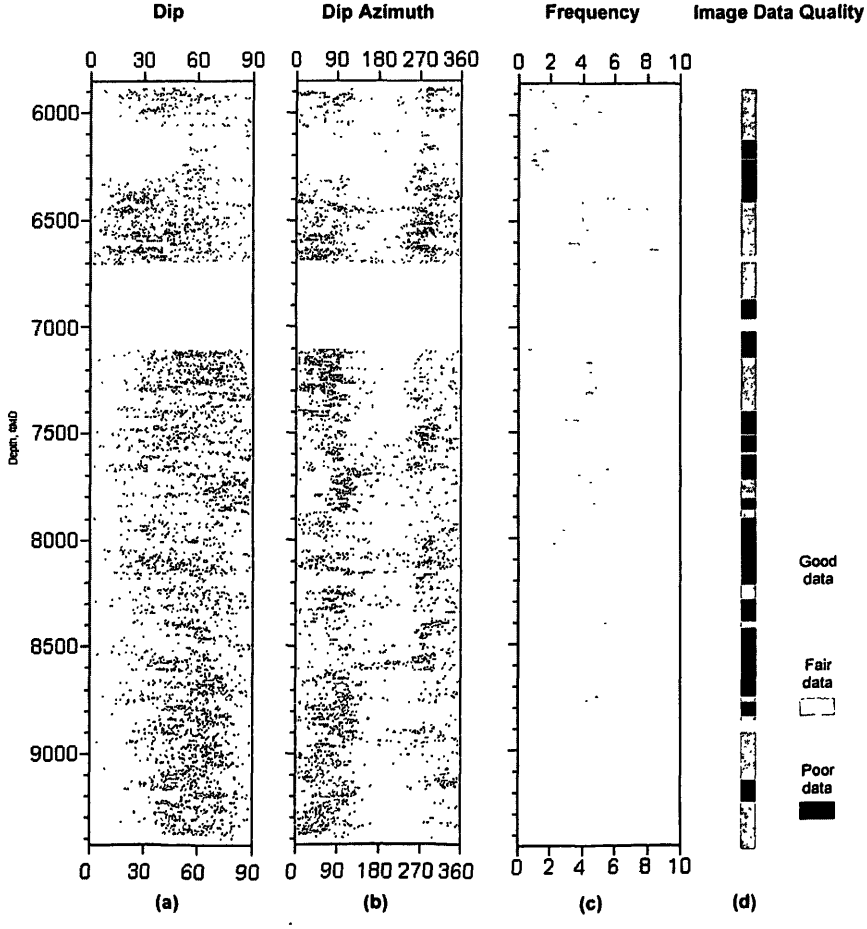


**Figure 2.** Preliminary results of the fracture analysis for well 38C-9 showing (a) fracture dips, (b) dip directions, (c) fracture frequency per foot, and (d) image data quality. The analysis and review is still ongoing and reflected by gaps and sparse fracture intervals. The light gray color in (a), (b) and (c) is used to emphasize the preliminary nature of these results. Image data quality (d) is shown where dark gray is poor image quality, intermediate gray is fair, and light gray is good image quality.

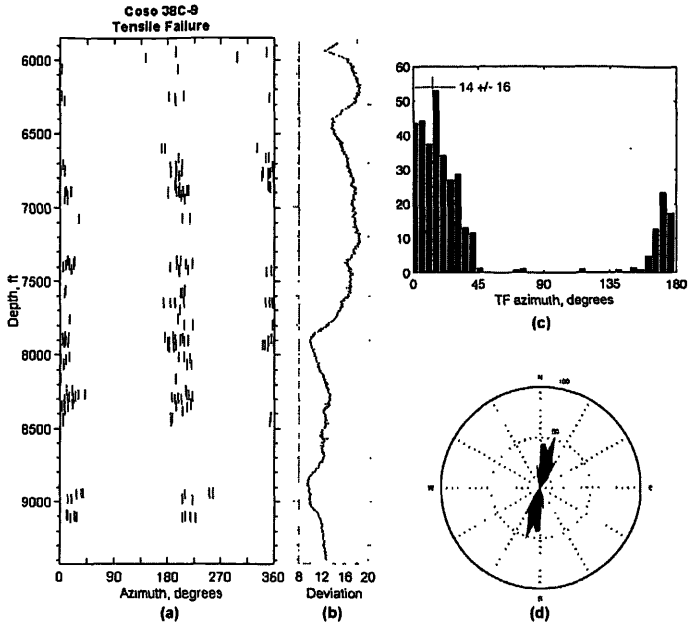


**Figure 3.** (a) Azimuth of tensile failure observed in well 38C-9 (vertical red bars). (b) Wellbore deviation in degrees with a gray line at 12°. (c) Histogram, and (d) rose diagram of tensile wall fracture orientation showing a consistent tensile fracture orientation at 14° ±16°azimuth of $S_{Hmax}$ in this near-vertical well.

The azimuthal orientations of the tensile fractures are displayed in the geographic reference frame in Figure 3. A statistical analysis of the azimuths of all observed failures in the well 38C-9 yields a tensile fracture orientation of 14° ±16°. 38C-9 is deviated more than 12° (Figure 3b) over most of the logged interval; therefore, as discussed previously the azimuth of wellbore failures may be rotated away from the $S_{Hmax}$ azimuth.

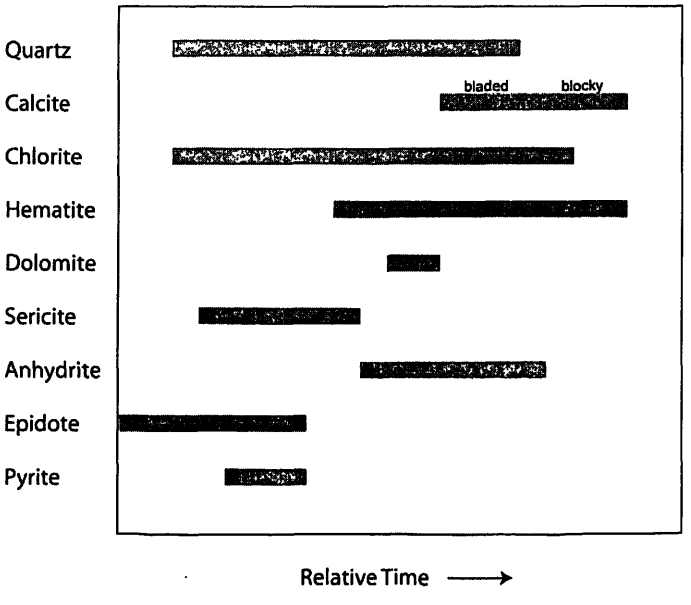


**Figure 4.** Vein mineral paragenesis showing the relative sequence of mineral deposition within Coso east flank fractures as determined from wellbore cuttings analyses.

## Petrologic Relationships

Detailed petrographic and petrologic analyses of several east flank wells have been completed and are reported elsewhere (Rose et al., 2003). Figure 4 summarizes a vein mineral paragenesis derived from these studies. It chronicles the deposition of minerals formed during hydrothermal events affecting the Coso east flank. Among the earliest minerals to deposit were quartz, epidote and chlorite, whereas the most recently deposited minerals were hematite and blocky calcite.

Fluid inclusions that were trapped when the veins were deposited reveal information about the depositional environment of those minerals. Shown in Figure 5 are the fluid-inclusion homogenization temperatures as a function of depth for east flank well 83-16. Each datum is a measure of the temperature at which the inclusion was formed within the vein mineral. It is evident that the epidote inclusions were formed during a previous era of geothermal activity when the reservoir temperature was somewhat higher than current temperatures. Interestingly, many of the calcite fluid inclusions record formation temperatures somewhat cooler than present day. Since calcite is the latest mineral deposited, this indicates that the temperatures of the rock and fluids within well 83-16 and possibly other east flank wells as well have increased since these inclusions were formed.

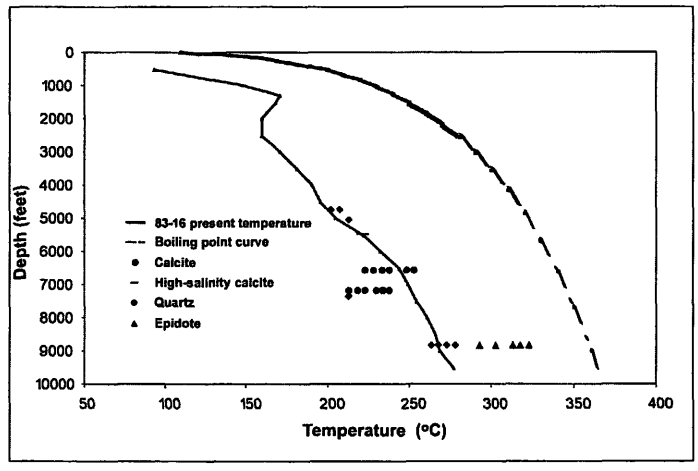


**Figure 5.** Plot of fluid-inclusion homogenization temperatures vs. depth showing that present day reservoir temperatures within well 83-16 are higher than temperatures recorded by calcite-hosted inclusions.

## Discussion

An understanding of the fracturing and stress state within a candidate EGS are essential for understanding and predicting the success or failure of subsequent reservoir stimulation experiments. The faults and fractures that are likely to be reopened upon hydraulic stimulation are those that are optimally oriented and critically stressed for shear failure. The preliminary orientation of the maximum horizontal stress, 14° +/- 16°, is within the range of horizontal stress orientations determined for other wells in the region. It is very close to the value obtained for 38A-9, which was 12° +/- 15°. The orientations of maximum horizontal stress for two other wells within the east flank, 83-16 and 38B-9 were determined to be somewhat more easterly at 50° and 65°,

respectively. Fractures that will become conductive upon hydraulic stimulation, either through normal or strike-slip faulting, will likely be relatively steeply dipping and have fracture dip azimuths within this range (12°– 65°).

An understanding of the vein mineralogy within a candidate EGS is also important for understanding the effects of hydraulic stimulation in hot tight wells. Faults in wells that are slightly conductive or were recently conductive can be distinguished from older, sealed faults by their mineral assemblages. The vein minerals in the more open faults are overlain with hematite and blocky calcite. It is possible that upon subsequent hydraulic fracturing experiments, only those calcite-laden faults will fail in shear. However, not all shear failure results in increased conductivity, as some faults seal upon shearing.

In addition to hydraulic stimulation, the success of chemical stimulation approaches may depend strongly on vein mineralization. For example, calcite-filled veins may be become more conductive upon the injection of condensate than veins filled with other more refractory minerals. Likewise, the success of chemical stimulants like acid or chelants will likely depend on the mineralogic make-up of the fractures.

## Conclusion and Summary

The work presented here is part of a 5-year project to test hydraulic, thermal and chemical stimulation concepts for creating an Enhanced Geothermal System within the east flank of the Coso geothermal reservoir. It extends our understanding of reservoir-stress and petrologic relationships, which will aid in the design of subsequent stimulation experiments.

A preliminary fracture/stress analysis was conducted for the recently drilled well 38C-9. EMI data were analyzed over the logged interval of 5,881-9,408 ft and naturally occurring fractures were analyzed in order to determine both fracture dip and azimuth. Most of the fractures were found to be steeply dipping with easterly dip azimuths. A subset of fractures within this wellbore dip steeply in a westerly direction. Drilling-induced tensile fractures were used to determine that the orientation of the maximum horizontal stress is 14° +/- 16°, although this is approximate because the data have yet to be corrected for wellbore deviation. Petrologic analyses of cuttings from several wells were used to construct a vein-mineral paragenesis of the Coso east flank. Fluid inclusion analyses of cuttings from well 83-16 revealed the temperatures of vein mineralization and indicate that this part of the reservoir is increasing in temperature.

## Acknowledgements

This project was supported by the U.S. Department of Energy Idaho Operations Office under grant DE-FC07-01ID14186. This support does not constitute an endorsement by the U.S. Department of Energy of the views expressed in this publication.

## References

Barton, C. A., S. Hickman, R. Morin, M. D. Zoback, and D. Benoit, 1998. Reservoir-scale fracture permeability in the Dixie Valley, Nevada, geothermal field, In: Proceedings, Twenty-Third Workshop on Geothermal Reservoir Engineering, SGP-TR-158, Stanford University, Stanford, California, January 26–28.

Barton, C. A., M. D. Zoback, and D. Moos, 1995. Fluid flow along potentially active faults in crystalline rock, *Geology*, 23 (8), pp. 683–686.

Mastin, L. G., 1988. Effect of borehole deviation on breakout orientations, *J. Geophys. Res.*, 93, 9,187–9,195.

Moos, D., and M. D. Zoback, 1992. *In situ* stress measurements in the NPR Hole, Savannah River Site, South Carolina: Final report to Westinghouse Savannah River Company, 200 pp.

Moos, D. and M. D. Zoback, 1990. Utilization of observations of well bore failure to constrain the orientation and magnitude of crustal stresses: Application to continental, Deep Sea Drilling Project and ocean drilling program boreholes, *J. Geophys. Res.*, v. 95, pp. 9,305–9,325.

Peska, P. and M. D. Zoback, 1995. Compressive and tensile failure of inclined well bores and determination of *in situ* stress and rock strength, *J. Geophys. Res.*, v. 100, no. 7, pp. 12,791–12,811.

Rose, P.E., S. Petty, C. Barton, J. McCulloch, J.M. Moore, K. Kovac, C. Kasteler, M.C. Adams, P. Wannamaker, S. Hickman, B. Julian, G. Foulger, D. Swenson, J. Sheridan, P. Spielman, B. Berard, K. Richards-Dinger, F. Monastero, (2003) Creation of an Enhanced Geothermal System through Hydraulic and Thermal Stimulation: DOE Technical Report for Quarter Ending December 31, 2002, DE-FC0701ID14186.

Sheridan, J., Kovac, K., Rose, P.E., Barton, C., McCulloch, J., Berard, B., Moore, J.M., Petty, S., and Spielman, P. (2003) *In situ* stress, fracture and fluid flow analysis—East Flank of the Coso Geothermal Field: Proceedings Twenty-Eighth Workshop on Geothermal Reservoir Engineering, Stanford University, SGP-TR-173.

Waldhauser, F., and W.L. Ellsworth, A double-difference earthquake location algorithm: Method and application to the northern Hayward fault, California, *BSSA*, *90* (6), 1353-1368, 2000.

Wu, H., and J.M. Lees, Three-dimensional *P* and *S* wave velocity structures of the Coso geothermal area, California, from microseismic travel time data, *JGR*, *104* (B6), 13217-13233, 1999.

Zoback, M. D., D. Moos, L. Mastin, and R. N. Anderson, 1985. Wellbore breakouts and in-situ stress, *J. Geophys. Res.*, v. 90, pp. 5,523–5,530.